

## Rare $B \rightarrow K^{(*)}\mu^+\mu^-$ decay in covariant quark model

---

**A. Liptaj<sup>\*a</sup>, S. Dubnička<sup>a</sup>, A. Z. Dubničková<sup>b</sup> and M. A. Ivanov<sup>c</sup>**

<sup>a</sup>*Institute of Physics, Slovak Academy of Sciences  
Bratislava, Slovakia*

<sup>b</sup>*Faculty of Mathematics, Physics and Informatics, Comenius University  
Bratislava, Slovakia*

<sup>c</sup>*Bogoliubov Laboratory of Theoretical Physics, Joint Institute for Nuclear Research  
Dubna, Russia*

*E-mail: [Andrej.Liptaj@savba.sk](mailto:Andrej.Liptaj@savba.sk)*

The covariant quark model with infrared confinement is presented. The model is used to describe the hadronic effects in the rare decay  $B \rightarrow K^{(*)}\mu^+\mu^-$  and predict value of several commonly used related observables.

*The European Physical Society Conference on High Energy Physics  
22–29 July 2015  
Vienna, Austria*

---

<sup>\*</sup>Speaker.

## 1. Introduction

Rare heavy hadron decays are nowadays a very active area of investigation with discovery potential. New high-luminosity machines today in operation allow for measurement of rare flavor-changing processes. Feynman diagrams of some of these processes may, in the loops, contain new hypothetical heavy particles. One reaction which might be sensitive to new physics is the  $B \rightarrow K^{(*)}\mu^+\mu^-$  decay. The process has been measured by [1, 2, 3, 4], where some results also include information about differential and angular distributions. As of now, the standard model (SM) is confirmed with some tensions ( $\sim 3\sigma$ ).

However any SM evaluation of the decay contains uncertainty related to the hadronic effects. The covariant quark model (CQM) is a Lagrangian-based effective field approach to hadronic interactions with limited number of free parameters. It is well suited to described the  $B \rightarrow K^{(*)}\mu^+\mu^-$  decay and check the agreement between the data and the SM.

## 2. Covariant quark model (mesons)

The CQM Lagrangian introduces meson-quark interaction as follows

$$\begin{aligned} \mathcal{L}_{\text{int}} &= g_M \cdot M(x) \cdot J_M(x), \quad J_M(x) = \int dx_1 \int dx_2 F_M(x, x_1, x_2) \cdot \bar{q}_{f_1}^a(x_1) \Gamma_M q_{f_2}^a(x_2), \\ F_M(x, x_1, \dots, x_n) &= \delta \left( x - \sum_{i=1}^n w_i x_i \right) \Phi_H \left( \sum_{i<j} ((x_i - x_j)^2) \right), \\ w_i &= m_i / \sum_{j=1}^n m_j, \quad \bar{\Phi}_H(-k^2) = \exp(k^2/\Lambda_M^2), \end{aligned} \quad (2.1)$$

where the meson field  $M$  interacts with a non-local quark current  $J_M$ . The symbol  $\Gamma_M$  corresponds to an appropriate string of Dirac matrices (depending on the particle spin) and the vertex function  $F_M$  is constructed in the way to be Lorentz invariant. It contains one free parameter  $\Lambda$  related to the size of the meson, the Gaussian shape is assumed for calculational convenience. The weights  $w_i$  are taken such as to match the quark-system barycenter with the meson position.

In addition to  $\Lambda$ s, the CQM contains as free parameters four constituent quark masses and one infrared cutoff, so in total  $N + 5$  parameters are needed to describe  $N$  hadrons. Their values (Table 1) are fixed by fits of the model to available experimental data. So-called compositeness condition [5, 6] is used to get a correct descriptions of hadrons as bound states of quarks and fix the values of the couplings  $g_M$ . It requires  $Z_M^{1/2} = 0$ , where the renormalization constant  $Z_M$  is interpreted as the matrix element between the physical state and the corresponding bare state. Making it zero implies that the physical state does not contain bare state and is therefore properly described as a bound state.

Parameter	$m_{u,d}$	$m_s$	$m_c$	$m_b$	$\lambda_{cutoff}$	$\Lambda_B$	$\Lambda_K$	$\Lambda_K^*$
Numerical value [in GeV]	0.241	0.428	1.67	5.05	0.181	1.96	1.02	0.75

**Table 1:** Parameters of the CQM model.

### 3. Computational techniques and infrared confinement.

A general Feynman graph with  $j$  external momenta,  $l$  loop integrations,  $m$  vertices and  $n$  quark propagators can be written as

$$\Pi(p_1, \dots, p_j) = \int [d^4k]^\ell \prod_{i=1}^m \Phi_{i_1+n}(-K_{i_1+n}^2) \prod_{i_3=1}^n S_{i_3}(\tilde{k}_{i_3} + \tilde{p}_{i_3}), \quad K_{i_1+n}^2 = \sum_{i_2} (\tilde{k}_{i_1+n}^{(i_2)} + \tilde{p}_{i_1+n}^{(i_2)})^2, \quad (3.1)$$

where  $\tilde{k}_i$  refers to the linear combination of loop momenta  $k_i$  and  $\tilde{p}_i$  to the linear combination of the external momenta  $p_i$ . We use the Schwinger representation of quark propagators

$$\tilde{S}_q(k) = (m + \hat{k}) \int_0^\infty d\alpha e^{-\alpha(m^2 - k^2)} \quad (3.2)$$

and make use of couple of smart operator identities to simplify the computations. The first one

$$\int d^4k P(k) e^{2kr} = \int d^4k P \left( \frac{1}{2} \frac{\partial}{\partial r} \right) e^{2kr} = P \left( \frac{1}{2} \frac{\partial}{\partial r} \right) \int d^4k e^{2kr}, \quad r = r(\alpha_i), \quad (3.3)$$

allows for an elegant loop momenta integration, the second one

$$\int_0^\infty d^n \alpha P \left( \frac{1}{2} \frac{\partial}{\partial r} \right) e^{-\frac{r^2}{a}} = \int_0^\infty d^n \alpha e^{-\frac{r^2}{a}} P \left( \frac{1}{2} \frac{\partial}{\partial r} - \frac{r}{a} \right), \quad a = a(\Lambda_H, \alpha_i), \quad (3.4)$$

simplifies the calculations following the trace evaluation: the derivative operator acts on unity instead of a more complex exponential function.

The final ingredient, the infrared cutoff, is introduced in relation with the integration over the Schwinger parameters. By inserting a unity in the form of a delta function, the multidimensional improper integral can be transformed to an integral over a simplex convoluted with only one improper integral. The cutoff is then applied on the upper integration limit

$$\Pi = \int_0^\infty d^n \alpha F(\alpha_1, \dots, \alpha_n) = \int_0^{\infty \rightarrow \frac{1}{\lambda^2}} dt t^{n-1} \int_0^1 d^n \alpha \delta\left(1 - \sum_{i=1}^n \alpha_i\right) F(t\alpha_1, \dots, t\alpha_n), \quad (3.5)$$

where  $F$  stands for the whole structure of a given diagram. Consequently,  $\Pi$  becomes a smooth function with thresholds in quark loop diagrams and corresponding branch points removed. Universal value for all processes  $\lambda = 0.181$  GeV is established and the integration is done numerically.

### 4. $B \rightarrow K^{(*)}\mu^+\mu^-$ decay

The hadronic effects for the process are parametrized by a set of form factors, depending on the spin of the final state particle.

- Three form factors in the case of a scalar particle ( $K$ ):

$$\left\langle P'_{[\bar{q}_3, q_2]}(p_2) | \bar{q}_2 O^\mu q_1 | P'_{[\bar{q}_3, q_1]}(p_1) \right\rangle = F_+(q^2) P^\mu + F_-(q^2) q^\mu, \quad (4.1)$$

$$\left\langle P'_{[\bar{q}_3, q_2]}(p_2) | \bar{q}_2 (\sigma^{\mu\nu} q_\nu) q_1 | P'_{[\bar{q}_3, q_1]}(p_1) \right\rangle = \frac{i}{m_1 + m_2} (q^2 P^\mu - q \cdot P q^\mu) F_T(q^2). \quad (4.2)$$

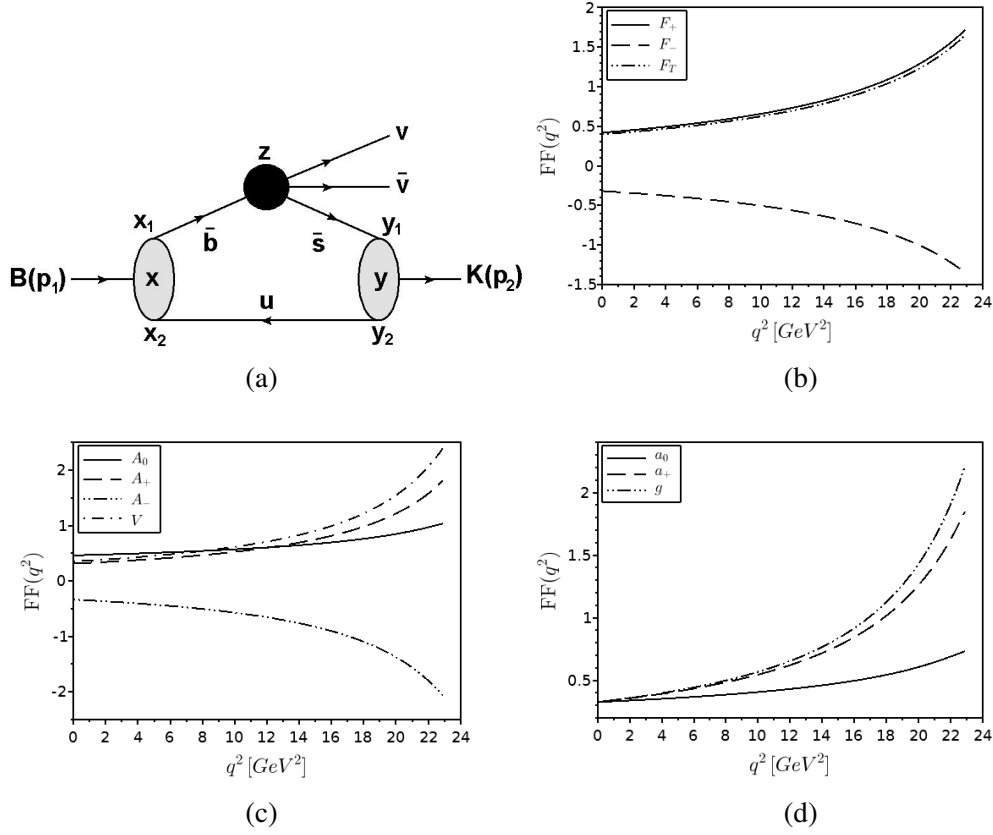


**Figure 1:**  $B \rightarrow K^{(*)}\mu^+\mu^-$ : Feynman diagram (a),  $B \rightarrow K$  form factors (b) and  $B \rightarrow K^*$  form factors (c-d).

- Seven form factors in the case of a vector particle ( $K^*$ ):

$$\langle V_{[\bar{q}_3, q_2]}(p_2, \varepsilon_2) | \bar{q}_2 O^\mu q_1 | P_{[\bar{q}_3, q_1]}(p_1) \rangle = \frac{\varepsilon_v^\dagger}{m_1 + m_2} \left[ -g^{\mu\nu} P \cdot q A_0(q^2) + P^\mu P^\nu A_+(q^2) + q^\mu P^\nu A_-(q^2) + i\varepsilon^{\mu\nu\alpha\beta} P_\alpha q_\beta V(q^2) \right], \quad (4.3)$$

$$\langle V_{[\bar{q}_3, q_2]}(p_2, \varepsilon_2) | \bar{q}_2 [\sigma^{\mu\nu} q_\nu (1 + \gamma^5)] q_1 | P_{[\bar{q}_3, q_1]}(p_1) \rangle = \varepsilon_v^\dagger \left[ - \left( g^{\mu\nu} - \frac{q_\mu q_\nu}{q^2} \right) P \cdot q a_0(q^2) + \left( P^\mu P^\nu - q^\mu P^\nu \frac{P \cdot q}{q^2} \right) a_+(q^2) + i\varepsilon^{\mu\nu\alpha\beta} P_\alpha q_\beta g(q^2) \right]. \quad (4.4)$$

The quark flavor transition and muon production is described by a four-fermion vertex using effective theory with local operators and Wilson coefficients. Their values are taken from the literature. The diagram of the process and the CQM form factors are shown on Fig 1.

## 5. Observables and results

We consider the cascade decay  $B \rightarrow K^{(*)}(\rightarrow K\pi)\mu^+\mu^-$  in order to fully explore the available experimental information (for kinematics see Fig 2(a)). We use the helicity approach to derive

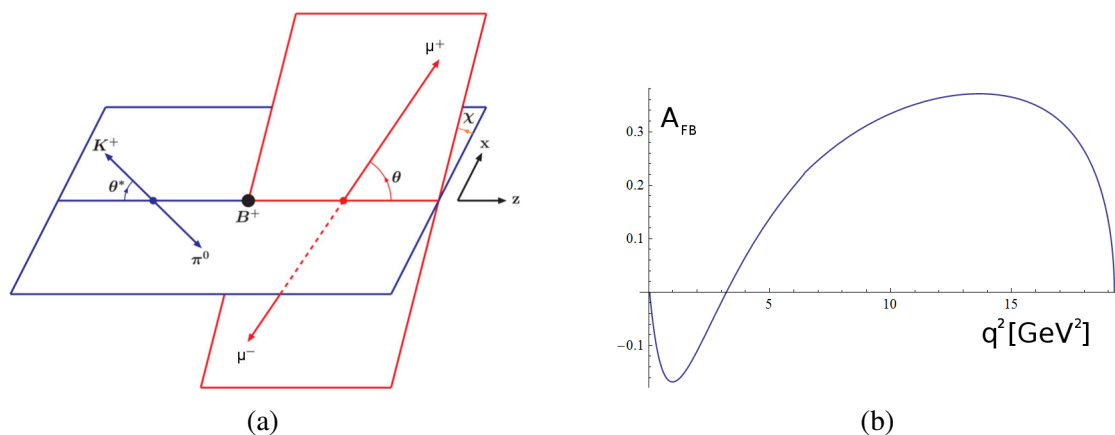


**Figure 2:** Kinematics of the  $B \rightarrow K^{(*)}(\rightarrow K\pi)\mu^+\mu^-$  decay (a) and the CQM prediction for  $A_{FB}$  (b).

the angular distributions and formulas for observables. They are expressed in terms of so-called helicity amplitudes (details in Ref. [7]).

The observables are chosen such as to be sensitive to possible new physic, but not sensitive to hadronic effects. In addition, they need to be well experimentally accessible. In this text we present our results on the branching fractions (Tab. 2), the lepton forward-backward asymmetry  $A_{FB}$  and the  $K^*$  longitudinal polarization  $F_L$ . The  $A_{FB}$  and  $F_L$  are coefficient  $q^2$ -dependent functions if front of the definite angular terms

$$\frac{1}{\Gamma} \frac{d^2\Gamma}{d\cos\theta_l dq^2} = \frac{3}{4}F_L(1 - \cos^2\theta_l) + \frac{3}{8}(1 - F_L)(1 + \cos^2\theta_l) + A_{FB}\cos\theta_l. \quad (5.1)$$

The predicted behavior of  $A_{FB}$  in the whole allowed kinematic range is shown in Fig. 2(b). In experiments, integrated forms of these observables are used (numerator and denominator integrated separately) and are measured in various  $q^2$  ranges. We chose the biggest one  $1\text{GeV}^2 < q^2 < 6\text{GeV}^2$  and present the comparison in Table 3 ( $K^*$  particle only).

## 6. Discussion and outlook

The CQM describes the measured data fairly well, maybe with the exception of the branching fraction for the  $B \rightarrow K\mu^+\mu^-$  reaction. In all cases the predictions have the correct order of magni-

Process	Branching fraction		Ref.
	CQM	Data	
$B \rightarrow K^*\mu^+\mu^-$	$1.27 \times 10^{-6}$	$(1.05 \pm 0.10) \times 10^{-6}$	[8]
$B \rightarrow K\mu^+\mu^-$	$7.18 \times 10^{-7}$	$(3.4 \pm 0.5) \times 10^{-7}$	[8]
$B \rightarrow K^*v\bar{v}$	$1.36 \times 10^{-5}$	$< 5.5 \times 10^{-5}$	[8]
$B \rightarrow Kv\bar{v}$	$0.60 \times 10^{-5}$	$< 4.9 \times 10^{-5}$	[8]
$B \rightarrow K^*\gamma$	$3.74 \times 10^{-5}$	$(4.21 \pm 0.18) \times 10^{-5}$	[9]

**Table 2:** Branching fractions for  $B \rightarrow K^{(*)}\mu^+\mu^-$  and similar processes.

	CQM	[1]	[2]	[3]
$\langle A_{FB} \rangle$	0.022	$0.26^{+0.27}_{-0.30} \pm 0.07$	$-0.06^{+0.13}_{-0.14} \pm 0.04$	$0.29^{+0.20}_{-0.23} \pm 0.07$
$\langle F_L \rangle$	0.75	$0.67 \pm 0.23 \pm 0.05$	$0.55 \pm 0.10 \pm 0.03$	$0.69^{+0.19}_{-0.21} \pm 0.08$

**Table 3:** Integrated observables  $\langle A_{FB} \rangle$  and  $\langle F_L \rangle$  for the  $B \rightarrow K^*\mu^+\mu^-$  decay.

tude and for what concerns angular observables in the  $K^*$  case, the experimental uncertainties are still important and situation is not conclusive.

A more detailed analysis concerning  $B \rightarrow K^{(*)}\mu^+\mu^-$  in the framework of the CQM is about to be published. It includes a larger set of observables (also so-called "clean" observables  $P_i$ ) and provides results in various bins.

Since the CQM proves to be a suitable tool for describing heavy hadron decays, we intend to apply it to other recently measured processes, e.g.  $B_s \rightarrow \Phi\mu^+\mu^-$  or  $B_s \rightarrow K_S K^*(892)^0$ .

## Acknowledgment

This work was supported by the Slovak Grant Agency for Sciences VEGA, Grant No. 2/0158/13 and the Slovak Research and Development Agency, contract No. APVV-0463-12.

## References

- [1] **Belle** Collaboration, J. T. Wei et al., *Measurement of the Differential Branching Fraction and Forward-Backward Asymmetry for  $B \rightarrow K^{(*)}\mu^+\mu^-$* , *Phys. Rev. Lett.* **103** (2009) 171801, [[arXiv:0904.0770](#)].
- [2] **LHCb** Collaboration, R. Aaij et al., *Differential branching fraction and angular analysis of the decay  $B^0 \rightarrow K^{*0}\mu^+\mu^-$* , *Phys. Rev. Lett.* **108** (2012) 181806, [[arXiv:1112.3515](#)].
- [3] **CDF** Collaboration, T. Aaltonen et al., *Measurements of the Angular Distributions in the Decays  $B \rightarrow K^{(*)}\mu^+\mu^-$  at CDF*, *Phys. Rev. Lett.* **108** (2012) 081807, [[arXiv:1108.0695](#)].
- [4] **BaBar** Collaboration, J. P. Lees et al., *Measurement of Branching Fractions and Rate Asymmetries in the Rare Decays  $B \rightarrow K^{(*)}l^+l^-$* , *Phys. Rev.* **D86** (2012) 032012, [[arXiv:1204.3933](#)].
- [5] A. Salam, *Lagrangian theory of composite particles*, *Nuovo Cim.* **25** (1962) 224–227.
- [6] S. Weinberg, *Elementary particle theory of composite particles*, *Phys.Rev.* **130** (1963) 776–783.
- [7] A. Faessler, T. Gutsche, M. A. Ivanov, J. G. Körner, and V. E. Lyubovitskij, *The Exclusive rare decays  $B \rightarrow K(K^*)\bar{\ell}\ell$  and  $B_c \rightarrow D(D^*)\bar{\ell}\ell$  in a relativistic quark model*, *Eur. Phys. J.direct* **C4** (2002) 18, [[hep-ph/0205287](#)].
- [8] **Particle Data Group** Collaboration, K. A. Olive et al., *Review of Particle Physics*, *Chin. Phys.* **C38** (2014) 090001.
- [9] **Heavy Flavor Averaging Group** Collaboration, Y. Amhis et al., *Averages of B-Hadron, C-Hadron, and tau-lepton properties as of early 2012*, [arXiv:1207.1158](#).